NJC

Cite this: *New J. Chem.*, 2011, **35**, 1020–1030

www.rsc.org/njc

PAPER

Pyridyl and pyridiniumyl β-diketones as building blocks for palladium(II) and allyl–palladium(II) isomers. Multinuclear NMR structural elucidation and liquid crystal behaviour†

María José Mayoral,[a] Pilar Cornago,[b] Rosa M. Claramunt[b] and Mercedes Cano*[a]

Received (in Montpellier, France) 28th November 2010, Accepted 8th March 2011
DOI: 10.1039/c0nj00938e

A series of novel β-diketone ligands bearing alkyloxyphenyl R = $C_6H_4OC_nH_{2n+1}$ and pyridyl substituents at 1 and 3 positions of the β-diketone core [$HL^{R(n)py}$] have been prepared and structurally characterized. The corresponding β-diketonate complexes [$Pd(\kappa^2\text{-}L^{R(n)py})_2$] were isolated as a mixture of *cis* and *trans* isomers each of them exhibiting the ligand in a NO- or OO-bidentate coordinative mode which were established by multinuclear NMR studies (^1H, ^{13}C and ^{15}N). However none of those characteristics were determining to achieve liquid-crystalline properties on the new complexes. By contrast reactions of the aforementioned ligands [$HL^{R(n)py}$] or those containing the pyridiniumyl substituent $[HL^{R(n)pyH}]^+$ towards the allyl–palladium fragment were successful to afford ionic metallomesogenic materials isolated as PF_6 salts of [$Pd(\eta^3\text{-}C_3H_5)(\kappa^2\text{-}HL^{R(n)py})][PF_6]$ (**I**) and [$Pd(\eta^3\text{-}C_3H_5)(\kappa^2\text{-}L^{R(n)pyH})][PF_6]$ (**II**) types. Structural characterization and mesomorphic properties were established by multinuclear NMR and the use of DSC and POM techniques. In complexes **I** and **II** the corresponding β-diketone ligands were coordinated as neutral bidentate NO-donor or *zwitterionic* OO-donor systems, respectively. Complexes of type **II** exhibit a range of the SmC mesophases significantly greater than that found in the type **I**.

Introduction

Coordination compounds constitute probably the largest category in the field of metallomesogenic materials. The interest of the current research on liquid crystal coordination compounds is directed to achieve a favourable mesomorphism avoiding the usual decomposition of the metallorganic systems at the temperatures frequently required to allow the supramolecular ordering of the mesophases.

In this context while the effects of the coordination geometry, the lateral substituents or their polar nature are investigated on many bis-β-diketonate metal systems,[1–12] the study of the introduction of a functional group on the molecular periphery of the ligand has not been commonly reported,[12] even though the formation of organic mesogenic materials from functionalized macrocyclic ligands is a subject of current interest.[2,13]

The β-diketonate core is an electron rich moiety in which the introduction of a polar group like pyridine could modify the dispersive forces and the intermolecular interactions. Taking into account the above considerations we thought that metal complexes containing long lateral chains and pyridine β-diketone type ligands could provide a new opportunity to reach metallomesogenic materials. In this point it is also interesting to note that most of the palladium β-diketonate complexes with two, three or four lateral chains display a square planar coordination geometry leading to discotic liquid crystal phases.[1–12]

On the other hand we have previously established that the metallic allyl–palladium fragment was able to induce a mesomorphic behaviour by coordination to mesomorphic or non-mesomorphic ligands leading to a stabilization of the mesophases. In those systems the electronic delocalization of the π–allyl system appears to be a favourable element to achieve the liquid crystalline properties.[14]

In this work we describe the study of novel palladium complexes based on β-diketone type ligands containing long chained alkyloxyphenyl substituents and pyridyl or pyridiniumyl groups at the 1 and 3 positions of the β-diketonate core, named [$HL^{R(n)py}$] and $[HL^{R(n)pyH}]^+$ (Scheme 1a). Two systems were selected to be studied: those of the type [$Pd(\kappa^2\text{-}L^{R(n)py})_2$] produced by coordination of two [$HL^{R(n)py}$] ligands to a Pd(II) center (Scheme 1b) and those obtained by coordination of the aforementioned ligands to the $[Pd(\eta^3\text{-}C_3H_5)]^+$ fragment (Scheme 1c).

[a] *Departamento de Química Inorgánica I, Facultad de Ciencias Químicas, Universidad Complutense de Madrid, E-28040 Madrid, Spain. E-mail: mmcano@quim.ucm.es; Fax: +34 91394 4352*
[b] *Departamento de Química Orgánica y Bio-Orgánica, Facultad de Ciencias, UNED, Senda del Rey 9, E-28040 Madrid, Spain. E-mail: rclaramunt@ccia.uned.es; Fax: +34 91398 8372*

† Electronic supplementary information (ESI) available: Tables S1–S8 and Fig. S1–S3. See DOI: 10.1039/c0nj00938e

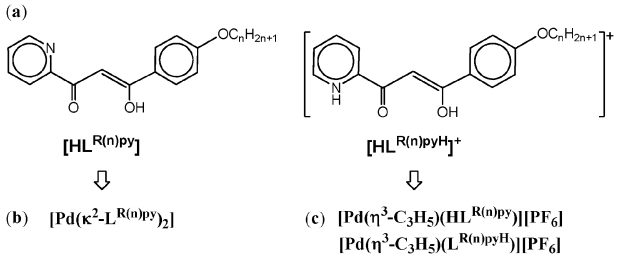

Scheme 1

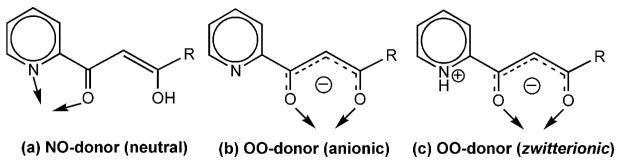

Fig. 1 Potential coordinative forms of (a) neutral $[HL^{R(n)py}]$, (b) anionic $[L^{R(n)py}]$ and (c) zwitterionic $[L^{R(n)pyH}]^+$ ligands

The work is directed to establish the ability of the selected β-diketones 1-(2-pyridyl)-3-(4-*n*-alkyloxyphenyl)propane-1,3-diones and the related salts 2-[3-(4-*n*-alkyloxyphenyl)-propane-1,3-dion-1-yl]pyridiniumyl chlorides to be coordinated as NO- or OO-chelating ligands (Fig. 1) towards Pd(II) or allyl–palladium fragment, so allowing us to study the influence of the metallic coordination environment on the mesomorphic behaviour of the complexes.

Thermal studies of all compounds are carried out in order to investigate their potential as liquid crystal materials.

Results and discussion

All the new compounds (**1–4**; **9–20**) described in this work are schematically presented in Table 1 including the number used to identify them. Schemes 2 and 3 depict the synthetic processes to obtain each type of compounds and the proposed

Table 1 Schematic formulation of the compounds

Compounds	*n*	Number
$[HL^{R(n)py}]$	12	**1**[a]
	14	**2**
	16	**3**
	18	**4**
$[HL^{R(n)pyH}]Cl$	12	**5**
	14	**6**
	16	**7**
	18	**8**[a]
$[Pd(\kappa^2\text{-}L^{R(n)py})_2]$	12	**9**[a]
	14	**10**
	16	**11**
	18	**12**
$[Pd(\eta^3\text{-}C_3H_5)(HL^{R(n)py})][PF_6]$ Type **I**	12	**13**
	14	**14**[a]
	16	**15**
	18	**16**
$[Pd(\eta^3\text{-}C_3H_5)(L^{R(n)pyH})][PF_6]$ Type **II**	12	**17**
	14	**18**[a]
	16	**19**
	18	**20**

[a] Selected compounds as representative examples for multinuclear NMR studies.

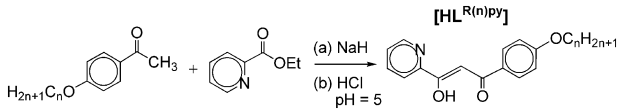

Scheme 2

molecular structure. The protonated β-diketonate pyridiniumyl derivatives isolated as chloride salts (**5–8**) described in a previous paper[15] are also included for comparative purposes.

Synthesis and characterisation

The ligands $[HL^{R(n)py}]$ (**1–4**) were readily prepared by reaction of the corresponding 4-*n*-alkyloxyacetophenone and 2-ethyl-picolinate in tetrahydrofuran. The reaction mixture was refluxed for 24 h (Scheme 2).

The related complexes $[Pd(\kappa^2\text{-}L^{R(n)py})_2]$ (**9–12**) were synthesized by reaction of the $Pd(Ac)_2$ with the corresponding ligands $[HL^{R(n)py}]$ in a NaH/dichloromethane media under reflux (Scheme 3a). All the complexes were isolated as yellow solids which were air-stable and soluble in common polar organic solvents.

The allyl–palladium derivatives $[Pd(\eta^3\text{-}C_3H_5)(HL^{R(n)py})][PF_6]$ (**13–16**) and $[Pd(\eta^3\text{-}C_3H_5)(L^{R(n)pyH})][PF_6]$ (**17–20**) were obtained when the dimer $[Pd(\mu\text{-}Cl)(\eta^3\text{-}C_3H_5)]_2$ was allowed to react with the neutral ligands $[HL^{R(n)py}]$ or with the related chloride salts $[HL^{R(n)pyH}]Cl$ in dichloromethane/acetone (Scheme 3b and c).

Spectroscopic studies

The ^{1}H-NMR spectra of ligands **1–4** were obtained in $CDCl_3$ solution. All of them exhibited a similar pattern (see ESI†). The multinuclear NMR study (^{1}H, ^{13}C and ^{15}N) of compound **1**, as a representative example, is reported in Table 2.

The 1-(2-pyridyl)-3-(4-*n*-alkyloxyphenyl)propane-1,3-dione ligands (**1–4**) can exist in solution as a pair of enol tautomers (Fig. 2a and b) and a keto form (Fig. 2c).[16] The ^{1}H-NMR spectra exhibit in all cases a similar pattern which is consistent with the enol form as the major one (>90%) (Fig. 2a and b) as deduced from the signal intensity ratios of the CH_2/CH protons. In addition, the combined use of ^{1}H and ^{13}C-NMR

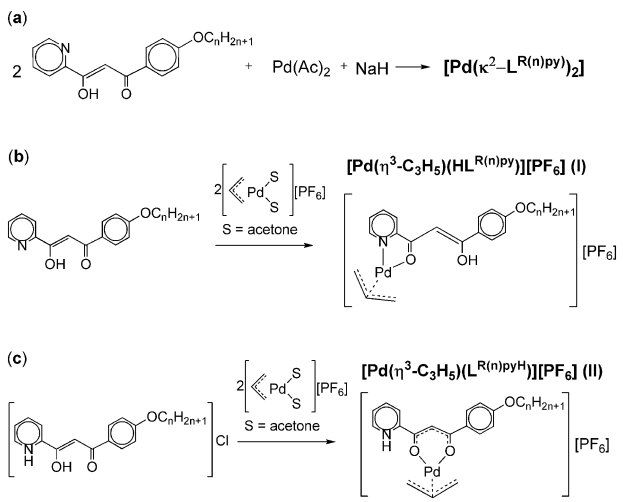

Scheme 3 Molecular structure of the palladium complexes.

Table 2 Selected NMR chemical shifts (δ in ppm) for **1** at 300 K

Atom[a]	Enol (94%) **1a** ≫ **1b**	Keto (6%) **1c**
C7		
$CDCl_3$	181.2	196.8
CPMAS	180.7	
H8/C8		
$CDCl_3$	7.52/92.9	4.80/48.0
CPMAS	91.1	
C9		
$CDCl_3$	187.1	193.6
CPMAS	187.0	
OH		
$CDCl_3$	16.64	
C2		
$CDCl_3$	152.6	152.7
CPMAS	151.2	
H3/C3		
$CDCl_3$	8.15/122.0	8.17/122.1
CPMAS	118.5	
H4/C4		
$CDCl_3$	7.87/137.1	7.89/137.0
CPMAS	135.4	
H5/C5		
$CDCl_3$	7.43/126.1	7.47/126.1
CPMAS	122.7	
H6/C6		
$CDCl_3$	8.71/149.1	8.62/149.0
CPMAS	151.2	
H_o/C_o		
$CDCl_3$	8.06/129.7	7.96/130.9
CPMAS	129.8	
H_m/C_m		
$CDCl_3$	6.96/114.4	6.93/114.3
CPMAS	112.4	
C_p		
$CDCl_3$	163.1	163.4
CPMAS	163.6	
C_{ipso}		
$CDCl_3$	127.8	127.3
CPMAS	126.2	
N1		
$CDCl_3$	−73.5	−66.3
CPMAS	−68.3	

[a] The numbering of the atoms is depicted in Fig. 2.

Table 3 Selected NMR chemical shifts (δ in ppm) for **8** at 323 K

Atom[a]	Enol (93%) **8a** ≫ **8b**	Keto (7%) **8c**
C7		
$CDCl_3$	174.1	n.o.
CPMAS	170.5	
H8/C8		
$CDCl_3$	8.11/96.0	4.82/n.o.
CPMAS	94.8	
C9		
$CDCl_3$	189.9	n.o.
CPMAS	188.6	
OH		
$CDCl_3$	16.48	
C2		
$CDCl_3$	149.9	n.o.
CPMAS	142.6, 144.4	
H3/C3		
$CDCl_3$	8.39/123.8	n.o.
CPMAS	118.2	
H4/C4		
$CDCl_3$	8.25/141.7	7.96/n.o.
CPMAS	134.1	
H5/C5		
$CDCl_3$	7.59/126.8	6.92/n.o.
CPMAS	127.1	
H6/C6		
$CDCl_3$	8.89/145.6	8.64/n.o.
CPMAS	150.1, 153.0	
H_o/C_o		
$CDCl_3$	8.26/130.8	7.91
CPMAS	130.0	130.6
H_m/C_m		
$CDCl_3$	7.00/114.8	6.91/114.3
CPMAS	113.5	
C_p		
$CDCl_3$	164.0	n.o.
CPMAS	165.6	
C_{ipso}		
$CDCl_3$	127.6	n.o.
CPMAS	124.2	
N1		
CPMAS	−181.6	

[a] The numbering of the atoms is depicted in Fig. 3; n.o. = not observed.

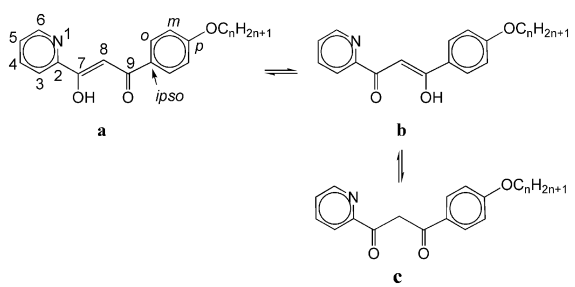

Fig. 2 Keto–enol equilibrium for [$HL^{R(n)py}$] (**1–4**).

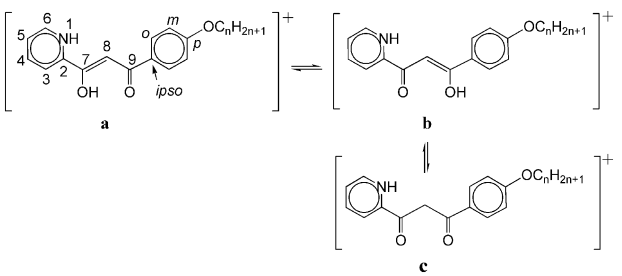

Fig. 3 Keto–enol equilibrium for [$HL^{R(n)pyH}$]Cl (**5–8**).

data point out to the **1a** form as the predominant enol (see Table 2 and further discussion for **8a**).[16]

The ^{1}H-NMR results of the 2-[3-(4-*n*-alkyloxyphenyl)-propane-1,3-dion-1-yl]pyridiniumyl chlorides (**5–8**) have been reported in a previous paper.[15] However a more complete study is now carried out by considering new data from ^{13}C and ^{15}N-NMR spectra taken for compound **8** (Table 3).

As in the related compound **1** the NMR data of the chloride salt **8** agree with the presence in solution of the enol and keto forms being the first ones the predominant (93%). In addition in this equilibrium **8a** is the main enol form (Fig. 3, Table 3).

We could establish from the 2D-NMR experiments [(^{1}H–^{1}H)gs-COSY, (^{1}H–^{13}C)gs-HMQC, (^{1}H–^{13}C)gs-HMBC] in $CDCl_3$ solution that both forms **1a** and **8a** are the major ones (Tables 2 and 3). We have been able to assign the corresponding

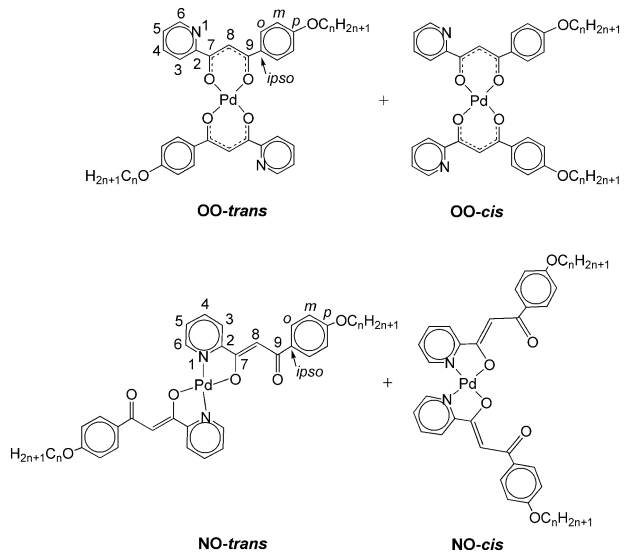

Fig. 4 Coordination and geometrical isomers of $[Pd(\kappa^2\text{-}L^{R(n)py})_2]$ (**9–12**).

signals to each ^1H and ^{13}C nuclei. On one side, C2 at 152.6/149.9 ppm is bonded to C7 which appears at 181.2/174.1 ppm; on the other side the C_{ipso} at 127.8/127.6 ppm is linked to C9 (carbonyl group C═O) at 187.1/189.9 ppm. In both cases the results agree with those previously found by us for related β-diketones.[16]

All palladium compounds containing 1,3-unsymmetrical disubstituted-propane-1,3-dionate units of the type $[Pd(\kappa^2\text{-}L^{R(n)py})_2]$ (**9–12**; Scheme 3a) were isolated as a mixture of coordination and geometrical isomers which exhibit a OO- or NO-coordination of the donor ligands and a *trans* or *cis* distribution (Fig. 4). The ratio of these isomers was determined by analysis of the multinuclear NMR results for compound **9** selected as representative example (Table 4).

In fact the $CDCl_3$ solution ^1H-NMR spectrum of **9** indicates the presence of four signals for each proton of the phenyl and pyridyl groups as well as for the C(8)H of the β-diketonate central core, those features suggesting the presence of the four isomers depicted in Fig. 4. In the mixture, the isomers are found in the following proportions: OO-*trans* (40%), OO-*cis* (10%), NO-*trans* (40%) and NO-*cis* (10%).

For each OO- or NO-coordinative form we have considered the *trans* geometry as the major one on the basis of the literature data,[17] as such a geometry avoids the steric congestion. However, weak signals from the *cis* forms were also observed in $CDCl_3$ solution, for all carbon and proton nuclei of each coordinative isomer (Table 4).

The four signals at 7.44 and 7.48/5.45 and 5.44 ppm of the C(8)H protons exhibit intensity ratios of 40 : 10/40 : 10. Similar features were found for the signals of the *meta* protons at 6.92 (40) and 6.91 (10)/6.74 (40) and 6.77 (10). In the case of the *ortho* protons at 7.91, 7.96 and 8.14 ppm the ratio is 40 : 10 : 50 indicating two overlapped signals at 8.14 ppm. Finally, the pyridyl protons show the same trendline (Table 4).

The IR spectra of the complexes **9–12** in the solid state (Fig. S1, ESI†) support the coexistence of the aforementioned four isomers, as they display a ν(CO) absorption band at 1693 cm^{-1} related to the presence in the ligand of an uncoordinated carbonyl group (NO-*trans* and NO-*cis* isomers, Fig. 4). In addition the second ν(CO) band at lower frequency, 1600 cm^{-1}, corresponds to a bidentate coordination involving the two carbonyl groups of the ligands (OO-*trans* and OO-*cis* isomers, Fig. 4).[18,19]

A final proof allowing us to support our conclusions comes out from the ^{15}N-NMR data of complex **9**. In the solid state the CPMAS spectra show the presence of an uncoordinated pyridine nitrogen at −66.9 ppm, together with a coordinated one at −158.7 ppm related to the OO or NO isomers, respectively. In $CDCl_3$ solution, the results agree with the presence of two major forms *via* NO- at −163.1 ppm and OO-coordination at −72.6 ppm, both assigned to the commonly more stable *trans* disposition, although a weak signal from the NO-*cis* isomer could also be observed (Table 4).

The coordination chemical shift $\Delta\delta$ ($\Delta\delta$ = δcomplex − δligand) for the NO-coordinated isomers is similar to that observed in palladium complexes containing the pyrazole ligand which exhibits a strong covalent Pd–N bond,[20] so suggesting a related bond for these isomers.

Reactions of the allyl–palladium fragment with the neutral ligands $[HL^{R(n)py}]$ were carried out in order to attain new organometallic compounds as potential liquid crystal materials. In this way complexes of the type $[Pd(\eta^3\text{-}C_3H_5)(HL^{R(n)py})][PF_6]$ (type **I**; **13–16**, Scheme 3b) were obtained.

Because of the versatile coordination of these ligands towards the palladium(II) metal centre observed in the above compounds $[Pd(\kappa^2\text{-}L^{R(n)py})_2]$ (**9–12**), we carried out the structural characterization of the new derivatives by multinuclear NMR (Table 5).

The ^1H-NMR spectra of the complexes **I** (Scheme 3b) in $CDCl_3$ solution at 300 K exhibit in all cases the corresponding signals of the ligands. For those compounds an enol coordinated form of the β-diketone core could be proposed on the basis of the signal at *ca.* 7.2–7.3 ppm corresponding to the C(8)H. A closer analysis of the NMR data of complex **14** as representative example of the series **I** shows the OH signal at 14.8 ppm, and the other ^1H, ^{13}C chemical shifts in agreement with the proposed structure involving a coordination through the *N*-pyridyl and *O*-keto atoms of the enol ligand (Scheme 3b). Here again the ^{15}N-NMR in the solid state has proved to be crucial to demonstrate that the pyridine nitrogen at −130.0 ppm is involved in the coordination around the palladium(II) center.[21]

If we analyze the allyl group, signals of *meso* (H_{meso}), *syn* (H_s) and *anti* (H_a) protons are clearly established and observed as three well separated signals at 5.80, 4.38 and 3.39 ppm, respectively, for **14**. Because this group exhibits a non-symmetrical environment the above results suggest *syn–syn* and *anti–anti* interchanges (Fig. 5), which are analogous to those described in the literature for related compounds.[22]

The protons of the pyridine group could also be clearly observed in their characteristic regions. In this context it is interesting to note that the signal of the H6 proton appears at 8.70 ppm, this value being similar to that found for the same proton in the related compound $[Pd(\kappa^2\text{-}L^{R(12)py})_2]$ (**9**).

Table 4 NMR chemical shifts (δ in ppm) for **9** at 300 K

Atom[a]	OO-*trans* (40%)	OO-*cis* (10%)	NO-*trans* (40%)	NO-*cis* (10%)
C7				
$CDCl_3$	182.5	181.9	199.8	199.7
CPMAS	186.6		200.1	
H8/C8				
$CDCl_3$	7.44/94.1	7.48/93.9	5.45/57.3	5.44/57.8
CPMAS			58.0	
C9				
$CDCl_3$	177.0	178.0	196.7	196.6
CPMAS	177.1		195.9	
C2				
$CDCl_3$	154.6	155.0	158.3	158.5
CPMAS	157.3		158.3	
H3/C3				
$CDCl_3$	7.98/121.7	8.05/121.9	7.87/122.2	7.87/122.3
CPMAS	123.1		124.1	
H4/C4				
$CDCl_3$	7.83/136.7	7.80/136.8	8.10/139.9	8.10/139.9
CPMAS	139.4		143.6	
H5/C5				
$CDCl_3$	7.36/125.2	7.37/125.3	7.60/127.0	7.60/126.9
CPMAS	125.4		126.5	
H6/C6				
$CDCl_3$	8.64/148.5	8.62/148.8	8.78/146.4	8.82/146.3
CPMAS	148.6		146.4	
H_o/C_o				
$CDCl_3$	7.91/129.5	7.96/129.7	8.14/130.6	8.14/130.7
CPMAS	132.3		134.9	
H_m/C_m				
$CDCl_3$	6.92/114.2	6.91/113.9	6.74/113.5	6.77/113.6
CPMAS	116.8/118.5		110.8	
C_p				
$CDCl_3$	162.1	162.0	162.40	162.37
CPMAS	162.9		162.9	
C_{ipso}				
$CDCl_3$	130.7	130.7	131.4	131.3
CPMAS	130.5		130.6	
N1				
$CDCl_3$	−72.6		−163.1	−163.4
CPMAS	−66.9		−158.7	
CH_3				
$CDCl_3$	0.86–0.89/14.1	0.86–0.89/14.1	0.86–0.89/14.1	0.86–0.89/14.1
CPMAS	14.6		15.2	
$(CH_2)_x$				
$CDCl_3$	1.27–1.86/22.7–31.9	1.27–1.86/22.7–31.9	1.27–1.86/22.7–31.9	1.27–1.86/22.7–31.9
CPMAS	24.2–34.1		24.2–34.1	
OCH_2				
$CDCl_3$	4.03/68.2	3.99/68.2	3.90/68.0	3.90/68.0
CPMAS	67.6		67.6	

[a] The numbering of the atoms is depicted in Fig. 4.

In order to support the NO-coordination of the enol form of the ligand, the IR spectra of all complexes **I** were recorded. All of them exhibit a ν(OH) absorption band at 3400–3450 cm^{-1}, which is characteristic of the enol form of the free β-diketones without intermolecular associations.[19]

On the other hand the ionic nature of complexes **I** was confirmed by the presence of the PF_6 counteranion bands at 842 ν(P–F) and 558 γ(F–P–F) cm^{-1},[18] and therefore with the neutral nature of the enol ligand in the complexes, so supporting their NO-coordination.

As a strategy to favour a bidentate OO-coordination of the ligand by blocking the *N*-pyridine group, the related cationic species $[HL^{R(n)pyH}]^+$ were also used towards the mentioned allyl–palladium fragment yielding to the new compounds $[Pd(\eta^3\text{-}C_3H_5)(L^{R(n)pyH})][PF_6]$ (type **II**; **17–20**, Scheme 3c) which were again structurally characterized by ^{1}H-NMR in all cases.

As they presented a similar pattern of signals with a C(8)H proton of the β-diketonate core at about 7.53 ppm, consistent with the enolate coordinative form (Scheme 3c), we decided to do a further study by ^{13}C- and ^{15}N-NMR which was carried out for **18** as representative example of this family. All chemical shifts gathered in Table 6 for this complex agree with such a coordination mode. In particular, it is interesting to note that the N1 chemical shift in the solid state is −185.6 ppm, a value close to that found in ligand **8** (Table 3) and typical of a protonated pyridine.

The allyl group shows three characteristic resonances corresponding to the *meso*, *syn* and *anti* protons. The two doublets from the *syn* and *anti* protons are at about 4.23 and

Table 5 Selected NMR chemical shifts (δ in ppm) for **14** at 323 K

Atom[a]	Chemical shifts (δ)
C7	
$CDCl_3$	185.3
CPMAS	189.8
H8/C8	
$CDCl_3$	7.23/94.1
CPMAS	92.1
C9	
$CDCl_3$	185.3/180.7
OH	
$CDCl_3$	14.80
C2	
$CDCl_3$	152.8
CPMAS	149.6
H3/C3	
$CDCl_3$	8.58/126.6
CPMAS	127.1
H4/C4	
$CDCl_3$	8.11/141.3
CPMAS	139.0
H5/C5	
$CDCl_3$	7.64/129.7
CPMAS	131.7
H6/C6	
$CDCl_3$	8.70/151.9
CPMAS	151.6
H_o/C_o	
$CDCl_3$	8.16/131.6
CPMAS	131.7
H_m/C_m	
$CDCl_3$	7.01/115.5
CPMAS	119.7
C_p	
$CDCl_3$	165.8
CPMAS	163.0
C_{ipso}	
$CDCl_3$	123.7
CPMAS	122.0
CH_2-allyl (H_s)	
$CDCl_3$	4.38/61.0
CPMAS	66.6/68.3
CH_2-allyl (H_a)	
$CDCl_3$	3.39/61.0
CPMAS	66.6/68.3
CH-allyl (H_{meso})	
$CDCl_3$	5.80/115.8
CPMAS	113.1/116.3
N1	
CPMAS	−130.0

[a] The numbering of the atoms is depicted in Fig. 5.

3.19 ppm, respectively, and the third multiplet signal at 5.68 ppm is assigned to the *meso* proton. The presence of a unique set of signals for each allyl proton suggests again the dynamic nature of the allyl group in the complex that allows the equivalence of the *syn–syn, anti–anti* protons despite the non-symmetrical environment produced by the β-diketonate ligand, similarly as it was described in the related complexes of type **I** (Fig. 5).

By considering the analogous results of the ^{1}H-NMR spectra in $CDCl_3$ solution of compounds **14** (family **I**) and **18** (family **II**) it becomes apparent that both correspond to the same species in solution. This feature could be explained on the basis of a fast exchange between the enol proton in **I** and the pyridiniumyl proton in **II**, through a neutral intermediate as depicted in Fig. 6.

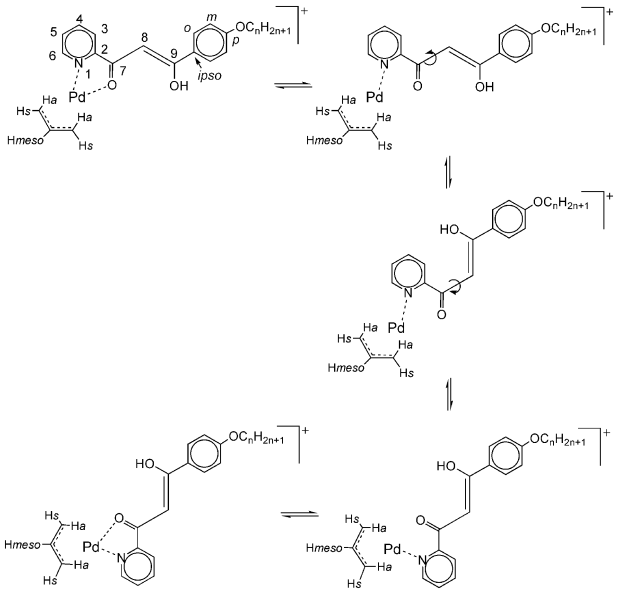

Fig. 5 *Syn–syn* and *anti–anti* interchanges in $CDCl_3$ solution for allyl–palladium complexes.

Table 6 Selected NMR chemical shifts (δ in ppm) for **18** at 323 K

Atom[a]	Chemical shifts (δ)
C7	
$CDCl_3$	185.4
H8/C8	
$CDCl_3$	7.53/94.6
C9	
$CDCl_3$	185.4
NH	
$CDCl_3$	14.60
C2	
$CDCl_3$	152.7
H3/C3	
$CDCl_3$	8.52/126.0
H4/C4	
$CDCl_3$	8.16/140.7
H5/C5	
$CDCl_3$	7.67/128.9
H6/C6	
$CDCl_3$	8.78/152.2
H_o/C_o	
$CDCl_3$	8.20/131.3
H_m/C_m	
$CDCl_3$	7.02/115.2
C_p	
$CDCl_3$	165.2
C_{ipso}	
$CDCl_3$	124.2
CH_2-allyl (H_s)	
$CDCl_3$	4.23[b]/61.0
CH_2-allyl (H_a)	
$CDCl_3$	3.19[c]/61.0
CH-allyl (H_{meso})	
$CDCl_3$	5.68/115.2
N1	
CPMAS	−185.6

[a] The numbering of the atoms is depicted in Fig. 5. [b] ^5J = 6.4 Hz. [c] ^3J = 11.8 Hz.

However from the multinuclear NMR studies of **14** and **18** in the solid state (Tables 5 and 6) we can conclude that for

complexes **I** the ligand $[HL^{R(n)py}]$ is in the enol form exhibiting a NO-coordination (Scheme 3b, type **I**). By contrast for complexes of type **II** with the $[HL^{R(n)pyH}]^+$ ligand an OO-coordinated enolate form is deduced (Scheme 3c, type **II**), giving rise in both cases to cationic species which were isolated as PF_6 salts.

IR spectra of type **I** complexes (**13–16**) in the solid state exhibit a ν(CO) absorption band at 1600 cm^{-1} and a ν(OH) band at *ca.* 3450 cm^{-1}. Both results agree with the presence of an enol form of the ligand in which the keto group is involved in the coordination leaving free the OH group. This feature supports a NO-coordination of neutral ligands $[HL^{R(n)py}]$ giving rise to cationic species. In agreement with this proposal the characteristic bands of the PF_6 ion observed at 842 ν(P–F) and 558 γ(F–P–F) cm^{-1} indicate its presence as a counteranion.[18]

For complexes of type **II** (**17–20**) again one ν(CO) band at 1602 cm^{-1} suggests that at least one carbonyl group is involved in the coordination of the ligands. In addition in all cases a strong and splitted band appears in the range of 3549–3415 cm^{-1}, which is attributed to ν(NH) of the pyridiniumyl group (Fig. S2, ESI†). On these basis a bidentate OO-coordination of the β-diketonate ligand is suggested. Therefore, in the cationic complexes $[Pd(\eta^3\text{-}C_3H_5)(L^{R(n)pyH})]^+$ (**II**) the ligand, which acts as bidentate β-diketonate should be in a *zwitterionic* form in order to maintain the neutral character of the complexes.

In summary we can establish the presence of two different structural environments for complexes **I** and **II** in the solid state, this fact being also reflected in the different liquid crystal behaviour observed in both cases (see the following discussion). In addition current photoluminescent studies performed on the complexes **14** (type **I**) and **18** (type **II**) show differences in the emission features in the solid state while the study carried out in dichloromethane solution displayed how the emission bands are similar in both cases.[23] These results were expected on the basis of the equilibrium described in Fig. 6.

Thermal studies

The thermal behaviour of all compounds was determined by using polarized-light optical microscopy (POM) and differential scanning calorimetry (DSC) techniques. The nature of the mesophases was confirmed by means of X-ray diffraction (XRD) at variable temperature. Table 7 summarises the thermal data of the compounds exhibiting liquid crystal behaviour (**13–20**).

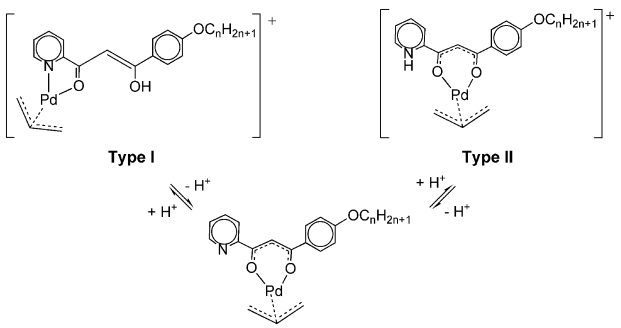

Fig. 6 Equilibrium of the allyl–palladium complexes in $CDCl_3$ solution.

Table 7 Phase behaviour of complexes **13–20** determined by DSC (scan rate: 10 K min^{-1})

		T/°C (ΔH/kJ mol^{-1})						
n		Cr	→	Cr′	→	SmC	→	I
12	**13**	·					180 (41.1)	·
14	**14**	·	76 (11.6)	·			173 (32.1)	·
16	**15**	·	90 (7.0)	·	155 (19.7)	·	172 (9.5)	·
18	**16**	·	87 (6.5)	·	144 (18.5)	·	153 (9.2)	·
12	**17**	·					174 (40.5)	·
14	**18**	·	84 (7.5)	·	158 (28.1)[a]	·	170 (28.1)[a]	·
16	**19**	·	78 (7.2)	·	107 (19.7)	·	160[b]	·
18	**20**	·			94 (18.9)	·	144 (5.2)	·

[a] Overlapped processes. [b] Temperature observed by POM.

β-Diketone ligands bearing a pyridyl substituent $[HL^{R(n)py}]$ (**1–4**) were not liquid crystal materials. In all cases the DSC thermograms show a single peak at *ca.* 80 °C corresponding to the endothermic transition from solid to the isotropic liquid.

In contrast to the mesomorphic behaviour of the related disubstituted-alkyloxyphenyl β-diketone ligands,[7,24] the absence of mesomorphism in compounds **1–4** requires an explanation which can be potentially established by considering that the length to width molecular ratio of these compounds, which is significantly lower than that of the related disubstituted ones, results inadequate to achieve the molecular ordering of the mesophases. On the other hand the expected increase in the molecular polarization, produced by the inclusion of the pyridyl group, should not be enough to compensate the molecular relationship mentioned above.

On the other hand all of the chloride salts previously reported that $[HL^{R(n)pyH}]Cl$ (**5–8**) displayed thermotropic polymorphism only consistent with crystal–crystal phase transitions.[15]

The complexes $[Pd(\kappa^2\text{-}L^{R(12)py})_2]$ (**9–12**) behave as non-mesomorphic materials suggesting that none of the isomers present in the complexes should exhibit liquid crystal behaviour. The presence of a mixture of compounds should not avoid observation of a liquid crystal behaviour if one of the components acts as mesomorphic.[25] We have inferred that, independently of the NO- or OO-coordination of the β-diketonate ligands in the *trans* or *cis* isomers, the square-planar bis-β-diketonate palladium(II) complexes yield to unfavourable molecular requirements to allow the supra-molecular order of the mesophases.

For the organometallic compounds studied in this work corresponding to the allyl–palladium systems the results were much more interesting. So, whereas the $[HL^{R(n)py}]$ (**1–4**) ligands were non-mesomorphic, their coordination to the $[Pd(\eta^3\text{-}C_3H_5)]^+$ fragment through the reaction with $[Pd(\eta^3\text{-}C_3H_5)(acetone)_2][PF_6]$ (Scheme 3b) gives rise to the new species $(HL^{R(n)py})][PF_6]$ (type **I**; **13–16**) which behave as liquid crystal materials in the cases **15** and **16** with extended alkyl chains (n = 16, 18 respectively).

The optical observations by POM in **15** and **16** confirm the presence of a single mesophase characterized as SmC on the basis of their typical *Schlieren* texture (Fig. 7).

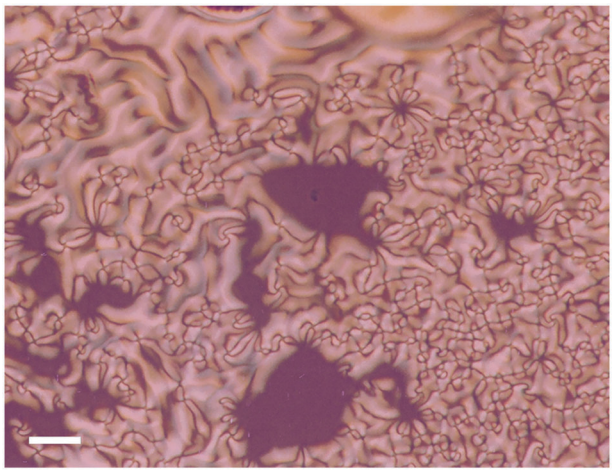

Fig. 7 Microphotograph of the SmC mesophase observed by POM of $[Pd(\eta^3\text{-}C_3H_5)(HL^{R(16)py})][PF_6]$ (**15**) at 160 °C on cooling (the white bar indicates 100 μm).

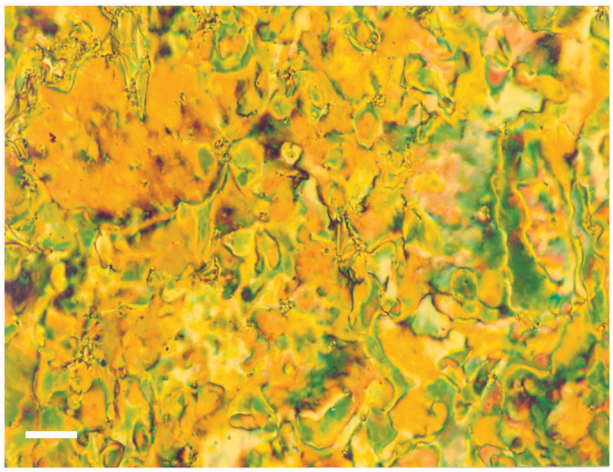

Fig. 8 Microphotograph of the SmC mesophase observed by POM of $[Pd(\eta^3\text{-}C_3H_5)(L^{R(14)pyH})][PF_6]$ (**18**) at 165 °C on heating (the white bar indicates 100 μm).

The related complexes **13** and **14** with shorter alkyl chains were not mesomorphic as deduced by POM, exhibiting in both cases an endothermic peak corresponding to the crystal-isotropic liquid phase transition observed on their DSC thermograms at 180 and 173 °C, respectively. Additionally, the thermogram of compound **14** shows a peak at 76 °C related to a preceding solid–solid phase transition.

In the DSC thermograms of complexes **15** and **16**, after a solid–solid phase transition at 90 and 87 °C, respectively, new peaks at 155 and 144 °C are attributed to the transformation from the solid to the SmC mesophase in agreement with the POM observations.

It was remarkable that on cooling the DSC thermograms of **13–16** did not show exothermic peaks with significant enthalpy values. This fact can be explained on the basis of the partial or extended decomposition suffered by the complexes on the first heating. That decomposition was less extended for the liquid crystals **15** and **16** which displayed the lower clearing temperatures. The appearance of the liquid-crystalline phase is favoured with the elongation of the alkyl chain, which also determines a decrease of both melting and clearing temperatures.

For the complexes of the type **II**, compound **17** (n = 12) did not show liquid crystal properties exhibiting only a single phase transformation from solid to the isotropic liquid at 174 °C. By contrast the other members of the series **18–20** (n = 14–18) are enantiotropic liquid crystals showing SmC mesophases which were identified by POM through their typical focal conic broken and *Schlieren* textures (Fig. 8). The DSC thermograms recorded on the first heating show two peaks corresponding to the solid-mesophase and mesophase-isotropic liquid phase transitions preceded by a solid–solid transition (Table 7). On cooling, the solidification process from the mesophase was not seen by DSC, but it was observable by POM.

For palladium-complexes **18–20** it should be noted that at the temperatures close to the clearing a slight decomposition is observed which is smaller as the length of the alkyl chain increases, in agreement with the decrease in the clearing temperature (Table 7). The partial decomposition causes a non-reproducibility of the thermal data in the successive heating cycles, this fact making difficult the observation of the mesophase on cooling from the isotropic liquid.

To determine the temperature of solidification, preventing decomposition, the samples were heated at temperatures slightly higher than those of the formation of the mesophase and then cooled. In this way the solid phase is reached and detected by DSC.

Again, the increase in the length of the alkyl chain leads to a decrease in the melting and clearing temperatures, avoiding the partial decomposition.

At this point of the discussion the effect of the coordination environment and the molecular shape in the liquid crystalline properties deserves a special comment.

For complexes **II** with the protonated ligand $[L^{R(n)pyH}]^+$ the bidentate OO-coordination involves the formation of a five-membered ring with an electronic delocalization similar to that observed in the related bis-β-diketonate palladium derivatives, while the protonated pyridyl group could probably not to be coplanar with the mentioned ring so introducing some distortion in the overall molecular geometry.

In order to achieve liquid crystal behaviour the balance between the cores and the molecular chains interactions is crucial. Thus, as it has been studied, when the contribution of the chains prevail, transition temperatures generally decrease as the chain length increases due to higher flexibility, making the interactions between the molecular cores more difficult. However, an opposite result was found if the core contribution is the determining factor.[26]

The main features observed in the complexes here studied agree with the first of these behaviours. Then, it is possible to suggest that the core–core interactions are disadvantageous compared to those of the alkyl chains, this effect being related to the absence of planarity of the molecular core.

Moreover, from the comparative study of the two families of complexes **I** and **II** we have been able to establish a selected design in order to improve the liquid crystal behaviour. In particular compounds **I** with a bidentate NO-coordination of

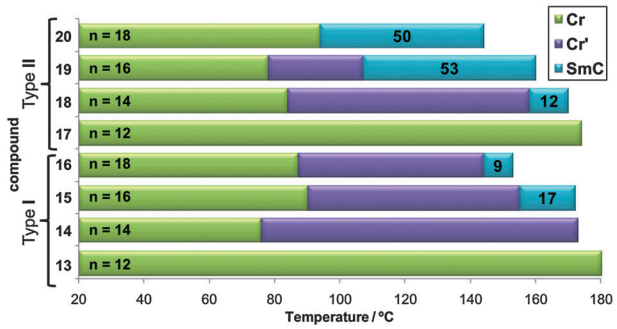

Fig. 9 Bar diagrams indicating the range of the phases (Cr, Cr′ and SmC) present in the complexes of the types **I** and **II**.

Table 8 X-Ray diffraction data

Complex	T/°C	Position (°)/2θ	d-spacing/Å	Miller indices (h k l)
15	160	2.6	34.3	(0 0 1)
		5.2	17.1	(0 0 2)
		7.7	11.4	(0 0 3)
		10.2	8.7	(0 0 4)
		20.0	4.5	[a]
19	130	2.4	37.1	(0 0 1)
		4.7	18.7	(0 0 2)
		7.0	12.6	(0 0 3)
		20.0	4.5	[a]

[a] Halo of the molten alkyl chains.

the ligand exhibit liquid-crystalline phases when they have extended alkyl chains, with n = 16 and 18 carbon atoms, while those of the type **II**, containing the *zwitterionic* OO-coordinated ligand, were liquid crystals in the cases of n = 14–18 carbon atoms. As it is depicted in Fig. 9 the compounds of type **II** have better mesomorphic properties exhibiting a range of the SmC mesophases significantly higher than that on the related complexes of type **I**.

Finally, selected metallomesogens were subjected to temperature dependent powder X-ray diffraction (XRD) measurements. The results are summarized in Table 8. XRD studies of the compounds confirm the smectic nature of the fluid phases observed by POM. Two set of reflections were observed in the diffractograms, one at small angles which display well-defined peaks in a 1 : 1/2 : 1/3 : 1/4 ratio from the (0 0 1), (0 0 2), (0 0 3) and (0 0 4) reflections corresponding to a lamellar structure, the other one consists in a diffuse halo at wide angles (*ca.* 4.5 Å) owing to the liquid-like order of the molten alkyl chains (Fig. S3, ESI†).

Experimental section

Materials and physical measurements

All commercial reagents were used as supplied. Commercial solvents were dried prior to use.

^{1}H-NMR spectra were performed at room temperature on a Bruker DPX-300 spectrophotometer (NMR Service of Complutense University) from solutions in $CDCl_3$. Chemical shifts δ are listed relative to Me_4Si using the signal of the deuterated solvent as reference (7.26 ppm), and coupling constants J are in hertz. Multiplicities are indicated as s (singlet), d (doublet), t (triplet), m (multiplet). The ^{1}H chemical shifts and coupling constants are accurate to ±0.01 ppm and ±0.3 Hz, respectively. In addition, the solution spectra of the compounds **1**, **8**, **9**, **14** and **18** were recorded, at 300 K save specified, on a Bruker DRX 400 (9.4 Tesla, 400.13 MHz for ^{1}H, 100.62 MHz for ^{13}C and 40.56 MHz for ^{15}N) spectrometer with a 5 mm inverse detection H–X probe equipped with a z-gradient coil for ^{1}H, ^{13}C and ^{15}N. Chemical shifts (δ in ppm) are given from internal solvents, $CDCl_3$ at 7.26 for ^{1}H and at 77.0 for ^{13}C. An external reference CH_3NO_2 (0.00) for ^{15}N-NMR was used.[27] 2D (^{1}H–^{1}H) gs-COSY and inverse proton detected heteronuclear shift correlation spectra, (^{1}H–^{13}C) gs-HMQC, (^{1}H–^{13}C) gs-HMBC, (^{1}H–^{15}N) gs-HMQC, and (^{1}H–^{15}N) gs-HMBC, were acquired and processed using standard Bruker NMR software and in a non-phase-sensitive mode.[28] Gradient selection was achieved through a 5% sine truncated shaped pulse gradient of 1 ms. Variable temperature experiments were recorded on the same spectrometer using a Bruker BVT3000 temperature unit to control the temperature. Solid state ^{13}C (100.73 MHz) and ^{15}N (40.60 MHz) CPMAS NMR spectra of **1**, **8**, **9**, **14** and **18** have been obtained on a Bruker WB 400 spectrometer at 300 K using a 4 mm DVT probe head and a 4 mm diameter cylindrical zirconia rotor with Kel-F end-caps. The non-quaternary suppression (NQS) technique to observe only the quaternary carbon atoms was employed.[29] ^{13}C-NMR spectra were originally referenced to a glycine sample and then the chemical shifts were recalculated to the Me4Si (for the carbonyl atom δ(glycine) = 176.1 ppm) and ^{15}N-NMR spectra to $^{15}NH_4Cl$ and then converted to nitromethane scale using the relationship: δ^{15}N(nitromethane) = δ^{15}N(ammonium chloride) − 338.1 ppm.

Elemental analyses for carbon, hydrogen and nitrogen were carried out by the Microanalytical Service of Complutense University.

IR spectra were recorded on a FTIR Thermo Nicolet 200 spectrophotometer with samples as KBr pellets in the 4000–400 cm^{-1} region: vs (very strong), s (strong), m (medium), w (weak).

Phase studies were carried out by optical microscopy using an Olympus BX50 microscope equipped with a Linkam THMS 600 heating stage. The temperatures were assigned on the basis of optic observations with polarised light.

Measurements of the transition temperatures were made using a Perkin Elmer Pyris 1 differential scanning calorimeter with the sample (1–4 mg) sealed hermetically in aluminium pans and with a heating or cooling rate of 10 K min^{-1}.

The X-ray diffractograms at variable temperature were recorded on a Panalytical X'Pert PRO MPD diffractometer in a θ–θ configuration equipped with a Anton Paar HTK1200 heating stage (X-Ray Diffraction Service of Complutense University).

Preparation of the [HL$^{R(n)py}$] compounds (1–4)

To a suspension of NaH (60 wt% in mineral oil, 15.3 mmol) in tetrahydrofuran was added 9.0 mmol of the corresponding 4-*n*-alkyloxyacetophenone and it was stirred at room

temperature for 30 min. Then 13.5 mmol of 2-ethylpicolinate in tetrahydrofuran were slowly added, and the reaction mixture was refluxed for 24 h. The solution was left to cool to room temperature and then was poured in *ca.* 400 mL of water and HCl solution (spec. grav. 1.19). The mixture was stirred for 24 h at room temperature. The pale yellow precipitate was filtered off and washed with *n*-hexane. Spectroscopic data are given for **1**. Data for the other homologues are essentially identical.

$[HL^{R(12)py}]$ (**1**). ν_{max}(KBr)/cm^{-1} 3389w (OH), 1602vs (C═O) + (C═C), 785m γ(CH)py.

Yields, elemental analysis and NMR data are given as ESI† (Tables S1 and S2).

Preparation of the $[HL^{R(n)pyH}]Cl$ salts (5–8)

The synthetic route for $[HL^{R(n)pyH}]Cl$ is shown in Scheme 1a. The detailed procedure and characterization by ^{1}H-NMR and IR has been previously reported by us.[15] New NMR data are also reported as ESI† (Table S3).

Preparation of the complexes $[Pd(\kappa^2\text{-}L^{R(n)py})_2]$ (9–12)

The corresponding $[HL^{R(n)py}]$ (0.30 mmol) and NaH (60 wt% in mineral oil, 0.60 mmol, 14.40 mg) were added to 75 ml of dichloromethane and stirred for 30 min. Palladium(II) acetate (0.15 mmol, 33.67 mg) which was dissolved in a small amount of dichloromethane was added to the reaction mixture and refluxed for 24 h. The hot reaction mixture was filtered over Celite and then was cooled to room temperature; the resulting orange precipitate was collected by filtration and then washed with hexane and dried *in vacuo*. Spectroscopic data are given for **9**. Data for the other homologues are essentially identical. Yields and elemental analysis are given as ESI† (Table S4).

$[Pd(\kappa^2\text{-}L^{R(12)py})_2]$ (**9**). ν_{max}(KBr)/cm^{-1} 1693s (C═C), 1601vs (C═O) + (C═C), 782m γ(CH)py.

Preparation of the complexes $[Pd(\eta^3\text{-}C_3H_5)(HL^{R(n)py})][PF_6]$ (13–16)

To a solution of $[Pd(\mu\text{-}Cl)(\eta^3\text{-}C_3H_5)]_2$ (100 mg, 0.273 mmol) in dry acetone (25 mL) was added $AgPF_6$ (138.1 mg, 0.546 mmol) under a nitrogen atmosphere. The mixture was stirred overnight in the absence of light and then filtered over Celite. The corresponding $[HL^{R(n)py}]$ (0.546 mmol) in dichloromethane (20 mL) was added to the resulting solution and let stirring overnight at room temperature. Then the solvent was removed *in vacuo* and the solid recrystallised in dichloromethane/hexane leading to the precipitation of a yellow solid, which was filtered off, washed with hexane and dried *in vacuo*. Spectroscopic data are given for **14**. Data for the other homologues are essentially identical.

$[Pd(\eta^3\text{-}C_3H_5)(HL^{R(14)py})][PF_6]$ (**14**). ν_{max}(KBr)/cm^{-1} 3410w (OH), 1600s (C═C) + (C═C), 780m γ(CH)py, 842vs ν(P–F), 558w γ(F–P–F).

Yields, elemental analysis and NMR data are reported in ESI† (Tables S5 and S6).

Preparation of the complexes $[Pd(\eta^3\text{-}C_3H_5)(L^{R(n)pyH})][PF_6]$ (17–20)

The synthetic process is analogous to that described above for **13–16** complexes, but in this case the corresponding $[HL^{R(n)pyH}]Cl$ salts were added. Spectroscopic data are given for **18**. Data for the other homologues are essentially identical.

$[Pd(\eta^3\text{-}C_3H_5)(L^{R(14)pyH})][PF_6]$ (**18**). ν_{max}(KBr)/cm^{-1} 3549m, 3487m, 3415s (NH), 1602s (C═C) + (C═C), 783m γ(CH)py, 845vs ν(P–F), 558w γ(F–P–F).

Yields, elemental analysis and NMR data are collected in ESI† (Tables S7 and S8).

Conclusions

The palladium(II) bis-β-diketonate complexes based on the strategically designed versatile ligands $[HL^{R(n)py}]$ which can coordinate in a bidentate NO- or OO-fashion were prepared and their molecular structures investigated. The complexes were isolated as a mixture of *trans* and *cis* isomers each of them having the ligand in one or other coordinative forms. The absence of liquid-crystalline properties indicate that none of the components of the mixture was liquid crystal, independently of all the variables found. By contrast the ionic complexes of the types $[Pd(\eta^3\text{-}C_3H_5)(HL^{R(n)py})][PF_6]$ (**I**) and $[Pd(\eta^3\text{-}C_3H_5)(L^{R(n)pyH})][PF_6]$ (**II**) containing the neutral ligand pyridyl β-diketone NO-coordinated or the related *zwitterionic* pyridiniumyl β-diketonate OO-coordinated proved to be metallomesogens exhibiting enantiotropic SmC mesophases independently of the different coordination environment around the metal. It appears that the π-delocalization of the allyl–palladium group was determining to produce lamellar mesophases, the better mesomorphic results being achieved for complexes of the type **II**. Therefore we can suggest that the allyl–palladium and the *zwitterionic* β-diketonate ligand are the best components in designing mesomorphic ionic compounds.

Acknowledgements

We thank the Spanish Ministry of Science and Innovation (grants no. CTQ2009-11880, CTQ2010-16122 and CTQ2010-19470), and UCM-Santander (GR58-08-910300) for the financial support.

Notes and references

1 B. Donnio, D. Guillon, R. Deschenaux and D. W. Bruce, *Comprehensive Coordination Chemistry II*, ed. J. A. McCleverty and T. J. Meyer, Elsevier, Oxford, 2003.
2 S. Kumar, *Chem. Soc. Rev.*, 2006, **35**, 83.
3 A. M. Giroud-Godquin and J. Billard, *Mol. Cryst. Liq. Cryst.*, 1981, **66**, 147; A. M. Giroud-Godquin and J. Billard, *Mol. Cryst. Liq. Cryst.*, 1983, **97**, 287; A. C. Ribeiro, A. F. Martins and A. M. Giroud-Godquin, *Mol. Cryst. Liq. Cryst. Lett. Sect.*, 1988, **5**, 133.
4 K. Ohta, A. Ishii, H. Muroki, I. Yamamoto and K. Matsuzaki, *Mol. Cryst. Liq. Cryst.*, 1985, **116**, 299; K. Ohta, H. Muroki, A. Takagi, I. Yamamoto and K. Matszaki, *Mol. Cryst. Liq. Cryst.*, 1986, **135**, 247; K. Ohta, O. Takenaka, H. Hasebe, Y. Morizumi, T. Fajimoto and I. Yamamoto, *Mol. Cryst. Liq. Cryst.*, 1991, **195**, 123; K. Ohta, O. Takenaka, H. Hasebe, Y. Morizumi, T. Fujimoto and I. Yamamoto, *Mol. Cryst. Liq. Cryst.*, 1991,

195, 13517; K. Ohta, H. Akimoto, T. Fujimoto and I. Yamamoto, *J. Mater. Chem.*, 1994, **4**, 61; K. Ohta, R. Higashi, M. Ikejima, I. Yamamoto and N. Kobayashi, *J. Mater. Chem.*, 1998, **8**, 1979.
5 B. Mühlberger and W. Haase, *Liq. Cryst.*, 1989, **5**, 251.
6 X. Yang, Q. Lu, S. Dong, D. Liu, S. Zhu, F. Wu and R. Zhang, *J. Phys. Chem.*, 1993, **96**, 6726.
7 S. N. Poelsma, A. H. Servante, F. P. Fanizzi and P. Maitlis, *Liq. Cryst.*, 1994, **16**, 675.
8 B. Heinrich, K. Praefcke and D. Guillon, *J. Mater. Chem.*, 1997, **7**, 1363.
9 B. K. Sadashiva and S. Rameska, *Mol. Cryst. Liq. Cryst.*, 1986, **141**, 19; K. Usha, K. Vijayan and B. K. Sadashiva, *Mol. Cryst. Liq. Cryst.*, 1987, **15**, 67; K. Usha and K. Vijayan, *Mol. Cryst. Liq. Cryst.*, 1989, **174**, 39; K. Usha, K. Vijayan and B. K. Sadashiva, *Mol. Cryst. Liq. Cryst.*, 1990, **185**, 1; K. Usha and K. Vijayan, *Mol. Cryst. Liq. Cryst.*, 1991, **201**, 17; K. Usha and K. Vijayan, *Mol. Cryst. Liq. Cryst.*, 1992, **220**, 772; V. Prasad and B. K. Sadashiva, *Mol. Cryst. Liq. Cryst.*, 1995, **268**, 89.
10 J. A. Campo, M. Cano, J. V. Heras, M. C. Lagunas, J. Perles, E. Pinilla and M. R. Torres, *Helv. Chim. Acta*, 2001, **84**, 2316.
11 C. K. Lai, H.-B. Pan, L.-F. Yang and K.-T. Liu, *Liq. Cryst.*, 2001, **28**, 97.
12 T. M. Swager, H. Zheng and B. Xu, *Chem. Mater.*, 1996, **8**, 907; J. Barbera, R. Gimenez, J. L. Serrano, R. Alcala, B. Villacampa, J. Villalba, I. Ledoux and J. Zyss, *Liq. Cryst.*, 1997, **22**, 265; K. Kishikawa, M. C. Harris and T. M. Swager, *Chem. Mater.*, 1999, **11**, 867; V. S. Bezborodov and V. F. Petrov, *Liq. Cryst.*, 1999, **11**, 867; O. Ihata, H. Yokota, K. Kanie, S. Ujtie and T. Kato, *Liq. Cryst.*, 2000, **27**, 69; M. R. Friedman, K. J. Toyne, J. W. Goodby and M. Hird, *Liq. Cryst.*, 2001, **28**, 901; W. Weissflog, H. Nadasi, U. Dunnemann, G. Pelzl, S. Diele, A. Eremin and H. Kresse, *J. Mater. Chem.*, 2001, **11**, 2748; C.-W. Chien, K.-T. Liu and C. K. Lai, *J. Mater. Chem.*, 2003, **13**, 1588.
13 S. Höger, J. Weber, A. Leppert and V. Enkelmann, *Beilstein J. Org. Chem.*, 2008, **4**, 1; S. H. Seo, T. V. Jones, H. Seyler, J. O. Peters, T. H. Kim, J. Y. Chang and G. N. Tew, *J. Am. Chem. Soc.*, 2006, **128**, 9264; W. Pisula, M. Kastler, C. Yang, V. Enkelmann and K. Müllen, *Chem.–Asian J.*, 2007, **2**, 51.
14 M. C. Torralba, J. A. Campo, J. V. Heras, D. W. Bruce and M. Cano, *Dalton Trans.*, 2006, 3918; M. C. Torralba, M. Cano, J. A. Campo, J. V. Heras, E. Pinilla and M. R. Torres, *J. Organomet. Chem.*, 2006, **691**, 765; M. Guedini, B. Panunzi and A. Roviello, *Liq. Cryst.*, 1998, **25**, 225.
15 M. J. Mayoral, P. Ovejero, J. A. Campo, J. V. Heras, E. Pinilla, M. R. Torres and M. Cano, *Inorg. Chem. Commun.*, 2009, **12**, 214.
16 P. Cornago, R. M. Claramunt, L. Bouissane, I. Alkorta and J. Elguero, *Tetrahedron*, 2008, **64**, 8089.
17 G. D. Fallon and B. M. Gatehouse, *Cryst. Struct. Commun.*, 1982, **11**, 1317; G. I. Zharkova, I. A. Baidina, S. A. Gromilov and I. K. Igumenov, *Koord. Khim.*, 1999, **25**, 690; K. Fukuyama, T. Tsukihara, K. Ohta and I. Yamamoto, *Tottori Daigaku Kogakubu Kenkyu Hokoku*, 1986, **16**, 42.
18 K. Nakamoto, *Infrared and Raman Spectra of Inorganic and Coordination Compounds*, Wiley, New York, 1986.
19 E. Pretsch, P. Bühlmann and M. Badertscher, *Structure Determination of Organic Compounds*, Springer-Verlag Berlin Heidelberg, Germany, 2009.
20 R. M. Claramunt, D. Sanz, G. Boyer, J. Catalán, J. L. G. de Paz and J. Elguero, *Magn. Reson. Chem.*, 1993, **31**, 791.
21 R. M. Claramunt, P. Cornago, V. Torres, E. Pinilla, M. R. Torres, A. Samat, V. Lokshin, M. Vales and J. Elguero, *J. Org. Chem.*, 2006, **71**, 6881.
22 J. Elguero, A. Fruchier, A. de la Hoz, F. A. Jalón, B. R. Manzano, A. Otero and F. Gómez-de la Torre, *Chem. Ber.*, 1996, **129**, 589; F. Gómez-de la Torre, A. de la Hoz, F. A. Jalón, B. R. Manzano, A. Otero, A. M. Rodríguez and M. C. Rodríguez-Pérez, *Inorg. Chem.*, 1998, **37**, 6606; F. Gómez-de la Torre, A. de la Hoz, F. A. Jalón, B. R. Manzano, A. M. Rodríguez, J. Elguero and M. Martínez-Ripoll, *Inorg. Chem.*, 2000, **39**, 1152; F. A. Jalón, B. R. Manzano and B. Moreno-Lara, *Eur. J. Inorg. Chem.*, 2005, 38.
23 M. J. Mayoral, P. Ovejero, J. A. Campo, J. V. Heras, E. Oliveira, B. Pedras, C. Lodeiro and M. Cano, *J. Mater. Chem.*, 2011, **21**, 1255.
24 K. Ohta, H. Muroki, K.-I. Hatada, A. Takagi, H. Ema, I. Yamamoto and K. Matsuzaki, *Mol. Cryst. Liq. Cryst.*, 1986, **140**, 163.
25 *Metallomesogens. Synthesis, Properties and Applications*, ed. J. L. Serrano, VCH, Weinheim, 1996.
26 C. K. Lee, K.-M. Hsu, C.-H. Tsai, C. K. Lai and I. J. B. Lin, *Dalton Trans.*, 2004, 1120.
27 R. M. Claramunt, D. Sanz, C. López, J. A. Jiménez, M. L. Jimeno, J. Elguero and A. Fruchier, *Magn. Reson. Chem.*, 1997, **35**, 35.
28 S. Berger and S. Braun, *200 and More NMR Experiments*, Wiley-VCH, Weinheim, 2004.
29 S. Braun, H.-O. Kalinowski and S. Berger, *150 and More Basic NMR Experiments*, Wiley-VCH, New York, 1998.

